Thin Functional Zeolite Layer Supported on Infrared Resonant Nano-Antennas for the Detection of Benzene Traces

Javier Nuñez, Arjen Boersma, Julien Grand, Svetlana Mintova, and Beniamino Sciacca

Infrared absorption spectroscopy is a powerful analytical tool that enables the identification of molecular species. The sensitivity of this technique, that is strongly limited by the small absorption cross-section of molecular vibration, can be greatly improved by resonant interaction with nano-antennas via the surface-enhanced infrared absorption (SEIRA) mechanism. However, most of the examples of SEIRA concern solid-state molecular layers adsorbed on the nano-antennas, while the detection of gas traces still remains elusive due to the spatial extent of the near-field that is used to amplify the molecular vibrations resonantly. Here, a hybrid system composed of a plasmonic nano-antenna array coupled with nanosized zeolite coating for detection of volatile organic compounds in the near field of the resonators is demonstrated. The concerted action of the coating and the nano-antennas enabled the authors to detect record traces of benzene (25 ppb) within 10 min. This approach may ultimately allow the fabrication of a compact system for rapid detection of pharmaceutical and biocompounds with high sensitivity and high selectivity.

1. Introduction

The detection of volatile organic compounds (VOCs) at trace levels (ppb to ppm) is of extreme importance in the field of environmental monitoring for health related matters. The European Air Quality Directive defines as mandatory the monitoring of certain VOCs, such as benzene in ambient conditions, and guideline values are provided by the World Health

J. Nuñez, Dr. A. Boersma
TNO Materials Solution
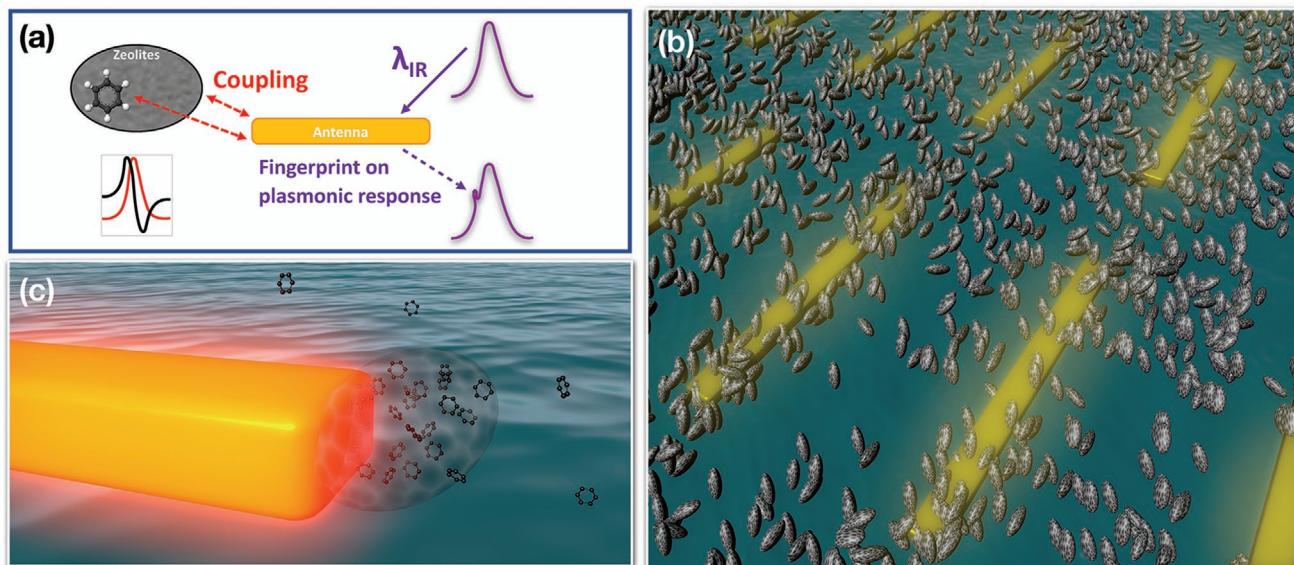High Tech Campus 25, 5656 AE Eindhoven, Netherlands

Dr. J. Grand, Dr. S. Mintova
ENSICAEN
UNICAEN
CNRS
LCS
Normandie Université
Caen 14050, France

Dr. B. Sciacca
CNRS
CINaM, Department of Nanomaterials
Aix-Marseille University
Marseille 13288, France
E-mail: beniamino.sciacca@univ-amu.fr

The ORCID identification number(s) for the author(s) of this article can be found under https://doi.org/10.1002/adfm.202101623.

Organization with an associated risk. The classical method for such measurements is gas chromatography, which is time-consuming, expensive, and not portable. Portable low-cost sensors have been developed for specific targets and are commercially available. Typically, these sensors either monitor changes such as conductance, strain, or absorption in a responsive material such as a polymer, or monitor the potential or the current in a chemical reaction.[1] These approaches can be very sensitive for a specific VOC targeting a concentration in the range from ppb to sub ppb, but they either lack versatility (developed for one specific target) and/or selectivity (discern a target in complex and unknown mixtures).

For a sensor to be able to detect a specific VOC in the ppb range, the sensing layer, and often the entire device, has to be designed and tailored toward a target substance (an analyte). Thereby, this approach hampers the versatility of the sensor, in the sense that the same sensor cannot be used to detect other analytes, since, in principle, the transducing mechanism is responsive only (or to a larger extent) to the targeted analyte. This is a consequence of detecting a target substance indirectly, that is, via an intermediate responsive material that imparts selectivity to the sensor, which is essential in real life applications.

Spectroscopic techniques in the mid infrared (3–20 µm) are able to detect directly the unique fingerprints of molecular transitions, therefore offering a valid alternative to the aforementioned approaches in terms of versatility and selectivity. The target substance with an active IR vibration can be detected from the unique fingerprint of its vibrational transitions, without the need for an intermediate transducer, or any prior knowledge.

However, versatility (ability to detect any species) and sensitivity (ability to detect low concentrations) are often incompatible in systems with a small footprint (cheap and portable). In fact, while IR spectroscopy allows for identification of chemical species in gas, liquid, and solid media, the light–matter interaction is extremely weak, thereby requiring long optical paths to boost the signal to noise ratio for applications where detection at ppb levels is required. This is due to the fact that the absorption cross-section of molecules in the IR is extremely small, being proportional to $\sigma_{abs} \propto a^3/\lambda$, with a being the molecule

Figure 1. a) SEIRA concept: near-field coupling between molecular/phonon transitions and optical resonances enables the amplification of the fingerprint. b) Gold nanorods array coated by zeolite nanocrystals able to trap benzene in regions where the near field enhancement is the highest (c).

characteristic size.[2] In the specific case of benzene the absorption cross-section of IR vibrational modes for one molecule is in the range of $\sigma_{abs} \approx 1$–10×10^{-20} cm^2.[3] Therefore, a large amount of molecules is needed to yield a signal above the noise level, in accordance with the Lambert–Beer's relationship. To keep a small footprint, it has been proposed to coat mid-IR waveguides or optical fibers with materials able to adsorb species of interest, thereby locally increasing the concentration.[4,5] However, this approach often lacks sensitivity that is required in many applications. One example is the monitoring of benzene at ppb or sub ppb levels, that remains challenging even if a separate pre-concentration step is employed.[6]

The use of resonant nano-antennas has proven to be effective in enhancing light absorption by organic molecules via the near field enhancement effect surface-enhanced infrared absorption (SEIRA).[7,8] The increase of sensitivity by 3–5 orders of magnitude compared to traditional IR absorption spectroscopy on films was reported.[9] Antennas are designed to have the resonance overlapping with the vibrational transition of target molecules as shown in **Figure 1**a.[10,11] This approach is very successful for detecting the vibrational fingerprint of solid state monolayers covering the nano-antennas. In such systems, the target molecules have to be very close to the antenna surface, where the field enhancement is the highest.[12] However, for low concentrated gases the probability of a molecule transiting within the strong field enhancement region can be very low. As an example, at a concentration of 25 ppb, there is roughly one molecule of benzene in a volume of 1 µm^3, whereas the mode volume of standard SEIRA nano-antennas is many orders of magnitude smaller ($\approx 10^{-3}$ µm^3). Therefore, for low concentrated volatile compounds that do not show significant adsorption on the antennas, the SEIRA approach alone is not suitable.

In this communication, we present a new approach that enables to extend the SEIRA toward the detection of gases at very lo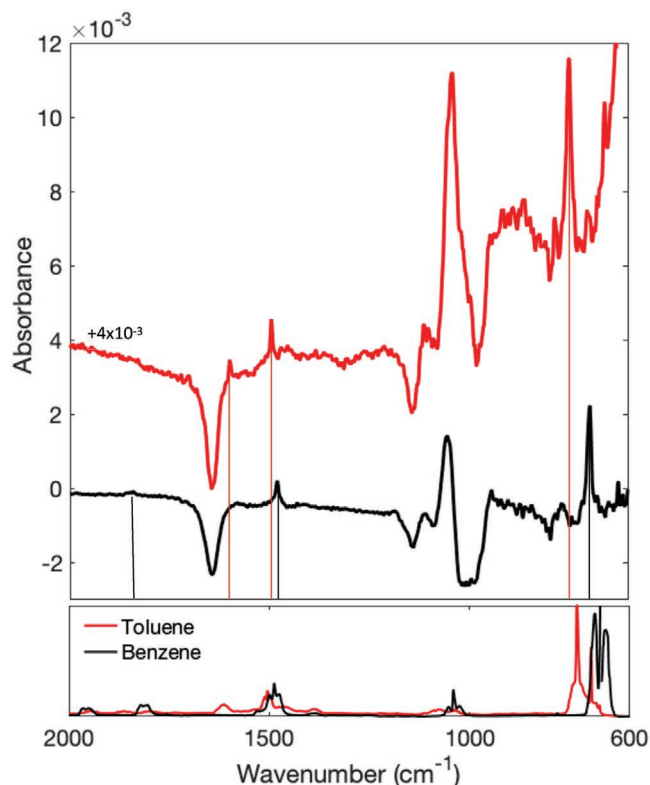w concentrations. The quick detection of benzene in the range of 20–30 ppb using a thin functional layer, and the capability to discriminate benzene from other VOCs such as toluene is demonstrated. To the best of our knowledge this sets a record for benzene detection using IR spectroscopy without external pre-concentration steps, considering that the concentrating role of the zeolite occurs in real-time with the measurement itself, as a one-step process. In addition, these values represent a great enhancement with respect to the low ppm range detection limit reported in the literature by using IR spectroscopy without a separate pre-concentration step, or with respect to the hundreds of ppb reported with IR tunable lasers.[6,13,14]

2. Results and Discussion

2.1. Zeolite Concentrating Coating

The development of an IR device for fast VOC detection of analytes in the ppb range requires a concerted approach in which the target molecules are trapped in close proximity of resonant nano-antennas hot spots, where the SEIRA can effectively take place. This can be achieved by coating the nano-antenna with a porous material able to capture and retain the analytes of interest. The porous material could be either organic such as polymers, hybrid such as metal-organic frameworks (MOF) or inorganic, such as zeolites or clays. Similar approaches were recently proposed by combining SEIRA nano-antennas with a MOF coating able to adsorb selectively CO_2 or CH_4. An improved detection limit for CO_2 in the order of several tens of ppm was reported.[15–17] This approach is limited to a certain extent due to the fact that the hybrid material used possesses many vibrational modes overlapping with molecules of interest (analytes).

Thus the desired "concentrating" coating should be suited to adsorb molecules with very low concentration and be compatible with the integration on the resonant nano-antennas. Zeolites

ADVANCED
SCIENCE NEWS
www.advancedsciencenews.com

ADVANCED
FUNCTIONAL
MATERIALS
www.afm-journal.de

Figure 2. IR spectra of benzene (black solid line) and toluene (red solid line) adsorbed on FAU coating. Bottom panel: the IR spectra of toluene and benzene in gas phase.

have little overlap with vibrational bands of the targeted molecules thanks to the pure inorganic nature.[18] Additionally, the zeolite with nanosized crystals enabled their deposition in a sub-100 nm zeolite film at low temperature via spin coating, which is compatible with resonant nano-antennas.[19,20] Among the available zeolites, the selection made in our study was based on: i) the pore size of the zeolites (that should be large enough to host benzene); ii) the hydrophobicity (to retain little water and adsorb predominantly VOCs); iii) the Henry's constant to adsorb VOCs at very low partial pressure;[21] and iv) the availability of the zeolites with nanosized dimensions stable in coating suspensions. Faujasite zeolite (sample denoted as FAU),[22] with a suitable pore diameter (0.72 nm) to adsorb benzene (0.5 nm)[23] and a crystal size of ≈20 nm, was selected for the current work.

Figure 2 shows the IR spectrum of benzene (black solid line) upon adsorption on FAU nanozeolite layer, while its spectrum in the gas form is shown in the bottom panel. Although the spectral shape of the molecular vibrations differs after adsorption, the peaks position, and relative intensity, are approximately unchanged. In particular, the characteristic aromatic C=C stretching (1480 cm^{-1}) and the out of plane C−H vibration (694 cm^{-1}) are clearly visible. It is important to notice a negative peak at 1645 cm^{-1}, corresponding to the loss of water still adsorbed in the zeolite structure despite extensive flushing with N$_2$ at room temperature. There are strategies, such as thermal desorption in vacuum, that are routinely used to desorb residual water from the zeolite pores, but those were not compatible with our experimental setup. Although the presence of

residual water in the pores has possibly a negative impact on the performance, it reproduces more realistic conditions.

Benzene exposure promotes rapid water desorption, probably due to its higher affinity toward the coating surface. The negative peaks at 1140 and 1000 cm^{-1} and the positive peak at 1053 cm^{-1} fall in the region of the T-O-T band of FAU (Figure 4d, blue curve), that is modulated by the desorption of water and adsorption of benzene (C−H in plane deformation at 1040 cm^{-1}).

Next, toluene was selected as an analyte to evaluate the selectivity of the sensors, that is, the capability to distinguish between molecules with very similar structures. We present in Figure 2 the IR spectra of toluene adsorbed in the FAU zeolite coating and in the gas phase. One can still discern between benzene and toluene even after adsorption in the zeolite coating. The use of zeolite coatings does not affect the quality of the IR spectra.

We evaluated the performance of the FAU coating by comparing the absorbance of the aromatic C=C stretching (1480 cm^{-1}) for a coating with a defined thickness with that of benzene in the gas phase for a given optical path. The concentration factor α was defined as

$$\alpha = \frac{C_{ref} d_{cell}}{A_{ref}} \frac{A_{sat}}{C_0 t_{coat}} \tag{1}$$

A_{ref} is the absorbance (for a specific peak) measured at concentration C_{ref} if no coating is used, and d_{cell} is the optical path of the cell. A_{sat} is the absorbance (of the same peak) measured in equilibrium conditions for a concentration C_0 when a zeolite coating with a thickness t_{coat} is present. For the FAU zeolite coating, α = 6×10^8 was estimated from Equation (1), meaning that in the linear regime (coating not saturated) under steady-state conditions, the concentration of benzene inside the coating is more than 8 orders of magnitude higher than outside (see Supporting Information for further details). The interactions are reversible upon N$_2$ delivery to the sensor, and the benzene desorbed from the zeolite coating (Figure S7, Supporting Information).

2.2. SEIRA Resonant Nano-Antennas

After identifying the best performing coating among those explored, we looked at a suitable nano-antennas design that is also a critical aspect of a device. Among the many possible designs, we fabricated gold nanorods in a phased array configuration. The individual nanorod is a nano-antenna itself with a resonance wavelength that depends on its characteristic size and on the refractive index of the supporting substrate. It is possible to use approximative scaling rules that predict the resonance wavelength from the length of the nanorods, given that nanorod width and height set.[24] Under some assumptions, a linear positive correlation of the resonance wavelength with the nanorod length is predicted. Therefore, nanorods are highly versatile, since they can be tuned to support resonances at any wavelength, by simply adjusting their length. By engineering the collective interaction in nanorod arrays, light scattered from individual nanorod can interfere constructively to yield a larger near field enhancement, and therefore a larger extinction in the far-field. The design of ordered arrays of nanorods has been shown to improve by one order of magnitude their performance compared to random arrays.[25]
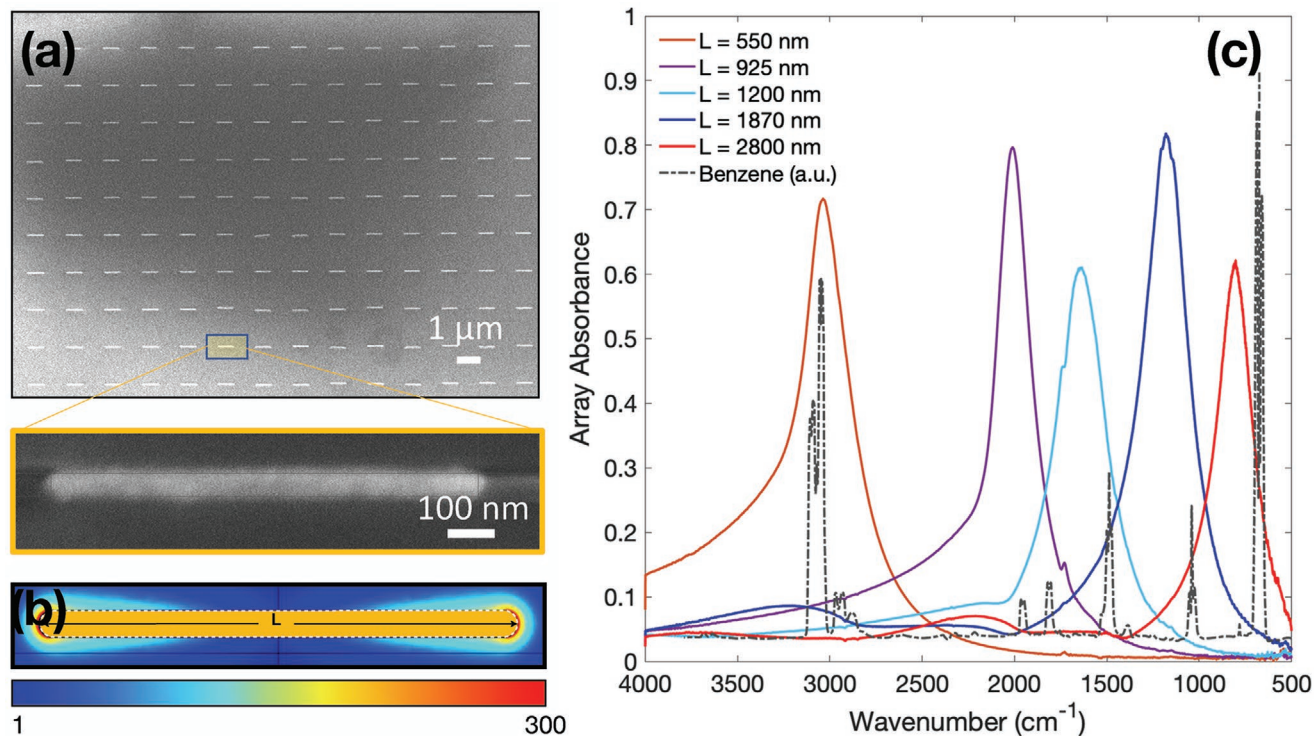
Figure 3. a) SEM image of a resonant nano-antenna array composed of phased gold nanorods. b) Field distribution at resonance, normalized by the incident field. c) IR spectra of nano-antenna array of different length overlapped with benzene spectrum (dotted spectrum).

Resonant nano-antennas consisting of gold nanorods arrays were prepared by e-beam lithography on a ZnSe substrate that remains fairly transparent to IR radiation until 15 µm, where VOCs possess the characteristic vibrational modes. Numerical simulations were employed to design a set of phased arrays resonant with several characteristic vibrational modes of benzene. The dimensions of nanorods and the periodicity of the array were chosen to maximize the near field enhancement. **Figure 3**a shows a representative SEM image of the fabricated arrays revealing nanorod size and pattern periodicity, which is very important to have an optimal response (in phase scattering). Figure 3b shows the electromagnetic field distribution simulated at resonance conditions, with a maximum near field enhancement in the order of 300. The experimental IR response of a set of arrays for a beam polarized along the long axis of the nanorods is presented in Figure 3c, showing the tunability of resonant features across a wide range of wavelengths, by mainly adjusting the nanorod length (see Supporting Information for further description). If the beam was polarized perpendicularly to the antenna axis (short length), no resonant features were visible, in accordance with theoretical predictions (Figure S3, Supporting Information); a clean ZnSe substrate was used as the reference.

2.3. Detection of Benzene Traces

Next, a FAU zeolite coating was used to trap and concentrate the targeted analyte in close proximity of the nano-antennas where the field enhancement is the highest (see Figure 3b).

The coating with an average thickness of 200 nm was prepared on the nano-antenna array via drop-casting. **Figure 4**a displays an SEM image of the sample overlaid with elemental compositions maps obtained via energy dispersive X-ray spectroscopy (EDX). A crack in the zeolite coating allows us to see the underlying gold nano-antenna array. Individual elemental composition maps are presented in Figure 4b. As expected Si, O, and Al coexist within the nanocrystals.

We selected a nano-antenna array with nanorod length of 1200 nm to assess the enhancement of the benzene band around 1480 cm^{-1}. We chose to focus on this band because the spectral feature of benzene was not influenced by other vibrational changes due to the coating-benzene interaction.

After deposition, a vibrational mode (1045 cm^{-1}) characteristic of FAU zeolite appears in the spectrum presented in Figure 4d (blue solid line). This mode lies outside the nano-antennas resonance and as expected it is not amplified.

The nano-antenna-zeolite was mounted in a gas cell in the optical path of IR light to assess its performance; mass flow controllers were used together with calibrated permeation tubes to obtain low concentrations of gases. The sample response upon exposure to 25 ppb of benzene is shown in **Figure 5**a and for different exposure times (IR light is polarized parallel to the nanorods long axis) in Figure 5b. A strong effect on the IR spectrum is observed within a few minutes on the bands that correspond to the interaction of benzene with the zeolite (940–1100 cm^{-1}). The spectral variation in the region of 1000 and 1700 cm^{-1} is consistent with what is observed for a FAU coating without antennas after benzene exposure (Figure 2) as described above. It is interesting to note that the
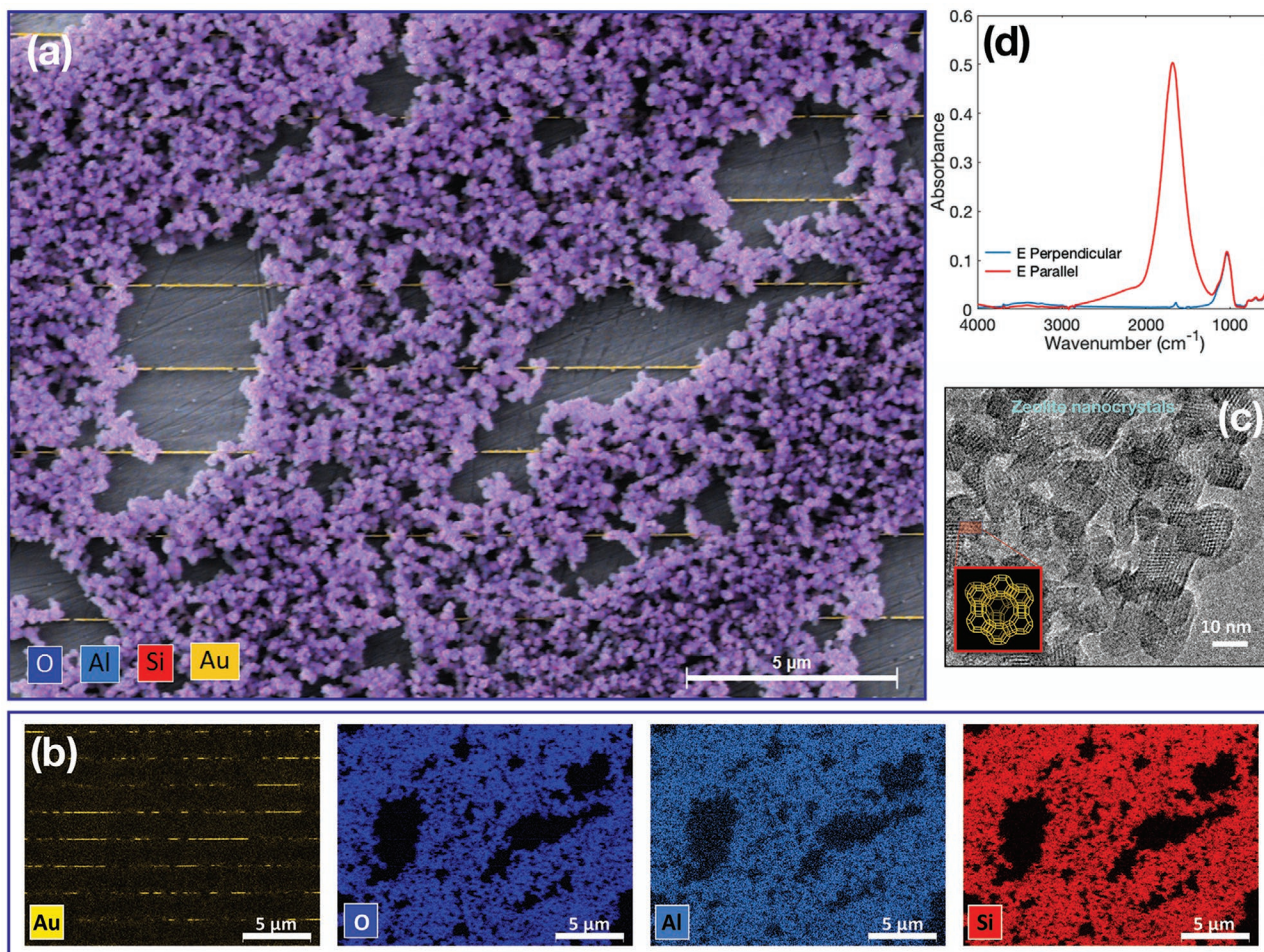
Figure 4. a) SEM image of a resonant nano-antenna array coated with FAU zeolite nanocrystals. b) The color corresponds to elemental distribution obtained by overlaying the EDX maps. The corresponding EDX spectrum is presented in Figure S5, Supporting Information. c) TEM image of FAU zeolite nanocrystals. The inset shows the FAU zeolite structure represented by the supercharge constructed by 6 sodalite cages connected via double-six rings. d) IR spectrum of 1200 nm long nano-antenna array coated with zeolite nanocrystals for parallel (red) and perpendicular polarization (blue), showing the resonance and the zeolite fingerprint.
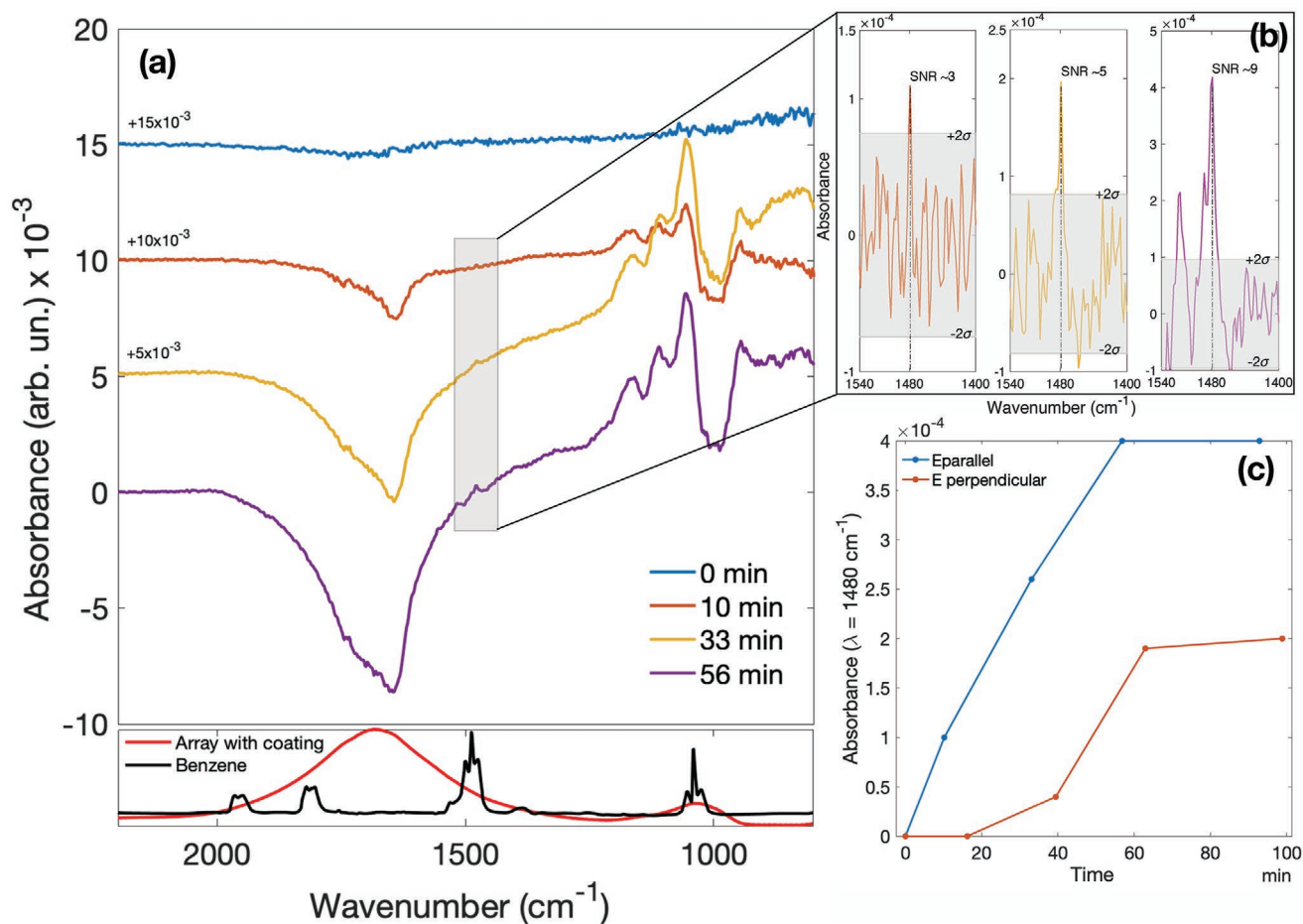
band around 1700 cm^{-1} corresponding to water is modulated by the nano-antennas resonance, as evidenced by the response for perpendicular polarization presented in Figure S8, Supporting Information.

Within 10 min, the characteristic aromatic C=C stretching peak of benzene (1480 cm^{-1}) is already above the noise (>3σ). The change of the intensity of the band at 1480 cm^{-1} as a function of time is presented in Figure 5c, both for parallel and perpendicular polarization.

In the framework of temporal coupled mode theory, the introduction of a loss channel as a result of the coupling with molecular vibrations (dark mode, weak compared to the nano-antennas mode) causes a perturbation of the coupling with external radiation. In under-coupled systems (radiation losses smaller than intrinsic absorption losses) it reduces absorption (electromagnetically induced transparency), while in over-coupled systems it increases it (electromagnetically induced absorption), as the ratio between radiative to non-radiative losses is reduced, driving the system toward the condition of critical coupling, that maximizes absorption.[10] Considering

that in our system radiation losses are larger than intrinsic absorption losses (over-coupled, see Figure S9, Supporting Information), the increase in absorbance upon benzene exposures (compared to perpendicular polarization) is consistent with predictions obtained in the framework of temporal coupled mode theory. The boost in sensitivity given by the resonant interaction of nano-antennas with the vibrational modes of benzene trapped within the near field enhancement volume is demonstrated in Figure 5. The concerted action of the FAU zeolite coating and the resonant nano-antennas enabled us to attain performance equivalent to a ≈120 m long optical path (see Supporting Information for further details). As shown in Figure 4d, the optical response of nano-antennas is strongly anisotropic. This enabled us to evaluate the individual contribution of the nanozeolite coating and SEIRA on the very same sample, by looking at the ratio of absorbance between parallel and perpendicular polarization in Figure 5c. The nano-antennas amplified the absorbance by a factor ≈3 as a consequence of resonant coupling, despite the overlap between the array resonance and the benzene mode was not optimal.

**ADVANCED
SCIENCE NEWS**
www.advancedsciencenews.com

**ADVANCED
FUNCTIONAL
MATERIALS**
www.afm-journal.de

Figure 5. a,b) IR response of nano-antenna-zeolite device upon exposure to 25 ppb of benzene at different time intervals. The spectrum at time 0 (after N_2 flushing, before benzene exposure) is used as a reference; the sample was placed in the cell during the entire experiment, to avoid artefacts due to inhomogeneity in the sample (nano-antenna and/or coating) and spatial dependence of the IR beam. c) Intensity of the peak at 1480 cm^{-1} as a function of time for parallel (blue) and perpendicular (red) polarization. Nano-antenna length: 1200 nm.

Although the contribution of nano-antennas is modest when compared to the zeolite concentration factor, it enabled us to detect 25 ppb of benzene in <10 min as opposite to ≈1 h. In addition to faster detection time, a larger SNR is obtained, which is especially important in the fabrication of portable devices.

Considering that the coating thickness was larger than the near-field enhancement, which is located near the nanorod ends, most of the coating did not interact with nano-antennas. As a consequence, the results shown in Figure 5c suggest that even thinner coatings could be employed to boost response time without sacrificing sensitivity. This, combined with nanophotonic designs, may improve the use of the substrate real estate in terms of field enhancement, and could further improve the performance.

3. Conclusions

We showed that by combining the nanozeolite concentrating coating with specifically designed IR nano-antennas was possible to use SEIRA for enhancing the light–matter interaction with the gas molecules used in this study (benzene and toluene). As a consequence, the detection of benzene down to 25 ppb was possible. In addition to the already mentioned strategies, the detection limit and SNR can be easily improved by using a N_2 cooled MCT detector as opposed to the DGTS detector used in this work, or by optimizing the thickness of the zeolite coating. Optimization of the zeolite coating with emphasis on the thickness, chemical composition, and porosity will be considered in the near future. Further perspectives for future works include the use of core-shell architectures[26] with the nano-antennas being the resonant core uniformly coated by a zeolite shell, and ultimately, employing monocrystalline nano-antennas to reduce ohmic losses applying the procedure previously reported.[27] These findings would have important effect in the design of portable systems for efficient detection of low concentrated gas pollutants in the atmosphere, especially in urban areas. Furthermore, the possibility to detect VOC at low concentrations can enforce guidelines regarding air quality standards.

2101623 (6 of 7)

Supporting Information

Supporting Information is available from the Wiley Online Library or from the author.

Conflict of Interest

The authors declare no conflict of interest.

Data Availability Statement

Research data are not shared.

Keywords

[1] L. Spinelle, M. Gerboles, G. Kok, S. Persijn, T. Sauerwald, *Sensors-Basel* **2017**, *17*, 1520.

[2] D. Dregely, F. Neubrech, H. G. Duan, R. Vogelgesang, H. Giessen, *Nat. Commun.* **2013**, *4*, 2237.

[3] T. Etzkorn, B. Klotz, S. Sorensen, I. V. Patroescu, I. Barnes, K. H. Becker, U. Platt, *Atmos. Environ.* **1999**, *33*, 525.

[4] R. Lu, G. P. Sheng, W. W. Li, H. Q. Yu, Y. Raichlin, A. Katzir, B. Mizaikoff, *Angew. Chem., Int. Ed.* **2013**, *52*, 2265.

[5] M. Sieger, B. Mizaikoff, *Anal. Chem.* **2016**, *88*, 5562.

[6] C. R. Young, N. Menegazzo, A. E. Riley, C. H. Brons, F. P. DiSanzo, J. L. Givens, J. L. Martin, M. M. Disko, B. Mizaikoff, *Anal. Chem.* **2011**, *83*, 6141.

[7] F. Neubrech, C. Huck, K. Weber, A. Pucci, H. Giessen, *Chem. Rev.* **2017**, *117*, 5110.

[8] X. Yang, Z. Sun, T. Low, H. Hu, X. Guo, F. J. Garcia de Abajo, P. Avouris, Q. Dai, *Adv. Mater.* **2018**, *30*, 1704896.

[9] F. Neubrech, A. Pucci, T. W. Cornelius, S. Karim, A. Garcia-Etxarri, J. Aizpurua, *Phys. Rev. Lett.* **2008**, *101*, 157403.

[10] R. Adato, A. Artar, S. Erramilli, H. Altug, *Nano Lett.* **2013**, *13*, 2584.

[11] T. Neuman, C. Huck, J. Vogt, F. Neubrech, R. Hillenbrand, J. Aizpurua, A. Pucci, *J. Phys. Chem. C* **2015**, *119*, 26652.

[12] R. Adato, H. Altug, *Nat. Commun.* **2013**, *4*, 2154.

[13] W. Chen, F. Cazier, F. Tittel, D. Boucher, *Appl. Opt.* **2000**, *39*, 6238.

[14] R. Sur, Y. Ding, R. B. Jackson, R. K. V. Hanson, *Appl. Phys. B* **2019**, *125*, 195.

[15] Y. H. Chang, D. Hasan, B. W. Dong, J. X. Wei, Y. M. Ma, G. Y. Zhou, K. W. Ang, C. Lee, *ACS Appl. Mater. Interfaces* **2018**, *10*, 38272.

[16] X. Y. Chong, Y. J. Zhang, E. W. Li, K. J. Kim, P. R. Ohodnicki, C. H. Chang, A. X. Wang, *ACS Sens.* **2018**, *3*, 230.

[17] H. Zhou, X. D. Hui, D. X. Li, D. L. Hu, X. Chen, X. M. He, L. X. Gao, H. Huang, C. Lee, X. J. Mu, *Adv. Sci.* **2020**, *7*, 2001173.

[18] A. Jentys, R. R. Mukti, H. Tanaka, J. A. Lercher, *Microporous Mesoporous Mater.* **2006**, *90*, 284.

[19] S. Mintova, J. P. Gilson, V. Valtchev, *Nanoscale* **2013**, *5*, 6693.

[20] T. Babeva, H. Awala, M. Vasileva, J. El Fallah, K. Lazarova, S. Thomas, S. Mintova, *Dalton Trans.* **2014**, *43*, 8868.

[21] M. J. Hwang, W. G. Shim, D. W. Ryu, H. Moon, *J. Chem. Eng. Data* **2012**, *57*, 701.

[22] H. Awala, J. P. Gilson, R. Retoux, P. Boullay, J. M. Goupil, V. Valtchev, S. Mintova, *Nat. Mater.* **2015**, *14*, 447.

[23] N. Y. Chen, *J. Phys. Chem.* **1976**, *80*, 60.

[24] L. Novotny, *Phys. Rev. Lett.* **2007**, *98*, 266802.

[25] D. Weber, P. Albella, P. Alonso-Gonzalez, F. Neubrech, H. Gui, T. Nagao, R. Hillenbrand, J. Aizpurua, A. Pucci, *Opt. Express* **2011**, *19*, 15047.

[26] B. Sciacca, S. A. Mann, F. D. Tichelaar, H. W. Zandbergen, M. A. van Huis, E. C. Garnett, *Nano Lett.* **2014**, *14*, 5891.

[27] B. Sciacca, A. Berkhout, B. J. M. Brenny, S. Z. Oener, M. A. van Huis, A. Polman, E. C. Garnett, *Adv. Mater.* **2017**, *29*, 1701064.